Weierstraß-Institut
für Angewandte Analysis und Stochastik

im Forschungsverbund Berlin e.V.

Preprint ISSN 0946 – 8633

Existence of bounded discrete steady state solutions of the van Roosbroeck system on boundary conforming Delaunay grids

K. Gärtner[1]

submitted: 25th September 2007

[1] Weierstrass Institute for Applied Analysis and Stochastics, Mohrenstrasse 39, 10117 Berlin, Germany
email: gaertner@wias-berlin.de

No. 1258
Berlin 2007

2000 *Mathematics Subject Classification.* 65M12, 35K65.

Key words and phrases. t Classification. 65M12, 35K65.
Key words and phrases. Reaction-diffusion systems, discrete bounded solutions, Delaunay grids, discrete weak maximum principle.

Edited by
Weierstraß-Institut für Angewandte Analysis und Stochastik (WIAS)
Mohrenstraße 39
10117 Berlin
Germany

Fax: + 49 30 2044975
E-Mail: preprint@wias-berlin.de
World Wide Web: http://www.wias-berlin.de/

EXISTENCE OF BOUNDED DISCRETE STEADY STATE SOLUTIONS OF THE VAN ROOSBROECK SYSTEM ON BOUNDARY CONFORMING DELAUNAY GRIDS

K. GÄRTNER *

Abstract. The classic van Roosbroeck system describes the carrier transport in semiconductors in a drift diffusion approximation. Its analytic steady state solutions fulfill bounds for some mobility and recombination/generation models. The main goal of this paper is to establish the identical bounds for discrete in space, steady state solutions on 3d boundary conforming Delaunay grids and the classical Scharfetter-Gummel-scheme. Together with a uniqueness proof for small applied voltages and the known dissipativity (continuous as well as space and time discrete) these discretization techniques carry over the essential analytic properties to the discrete case. The proofs are of interest for deriving averaging schemes for space or state dependent material parameters, which are preserving these qualitative properties, too. To illustrate the properties of the scheme 1, 4, 16 elementary cells of a modified CoolMOS like structure are depleted by increasing the applied voltage until steady state avalanche breakdown occurs.

2000 Mathematics Subject Classification. 65M12, 35K65.
Key words and phrases. Reaction-diffusion systems, discrete bounded solutions, Delaunay grids, discrete weak maximum principle.

1. Introduction. The analytic problem is well known. It is treated with different techniques and assumptions on data [1, 2, 3, 4, 5]. For the purpose of establishing discrete bounds it is convenient to follow Markowich [4]. The central assumptions made to introduce the finite volume space discretization are:
Gauss's theorem holds and boundary conforming Delaunay meshes cover the bounded polyhedral domain $\mathbf{\Omega} = \cup_i \mathbf{\Omega}_i$, $\mathbf{\Omega}_i$ a subdomain containing one material.
The first assumption is met by the known analytical smoothness results, the second one is a research topic in its own. It weakens assumptions like 'a mesh of acute type', on which the 2d results of Zlamal [6] are based. These results can be extended in more detail to relevant 3d situations.
The van Roosbroeck system, supplemented with boundary conditions, is discretized in the form

$$-\nabla \cdot \epsilon \nabla w = C - n + p, \tag{1.1}$$

$$\frac{\partial n}{\partial t} - \nabla \cdot n_i \mu_n e^{w} \nabla e^{-\phi_n} = R, \tag{1.2}$$

$$\frac{\partial p}{\partial t} - \nabla \cdot n_i \mu_p e^{-w} \nabla e^{\phi_p} = R, \tag{1.3}$$

where the symbols have the usual meaning (w - electrostatic potential, $n = n_i e^{w-\phi_n}$ - electron density, $p = n_i e^{\phi_p - w}$ - hole density, ϕ_n, ϕ_p quasi-Fermi potentials), and $R = r(x,n,p)(n_i^2 - np)$ (recombination / generation rate) with $r(x,n,p) > 0$ is assumed to hold. The intrinsic carrier densities (n_i) are supposed to be constant on each subdomain $\mathbf{\Omega}_i$, hence density like functions are 'measured' in n_i. The dielectric permittivity ϵ_i and the mobilities ($\mu_{n,p} > 0$) are assumed to be bounded, sufficiently

* Weierstrass Institute for Applied Analysis and Stochastics, Mohrenstr. 39, 10117 Berlin, Germany (gaertner@wias-berlin.de).

smooth functions in all arguments on each subdomain $\mathbf{\Omega}_i$ with discontinuities at subdomain boundaries. Potentials have the natural unit 'thermal voltage'. Einstein relations and Boltzmann statistics are used and the time derivatives vanish.

A summary with respect to the used properties of Delaunay grids and Voronoi diagrams follows in the next section together with the introduction of the discretization scheme. Section three deals with the Scharfetter-Gummel-scheme on simplex grids and establishes the existence of bounded discrete steady state solutions. Finally an example with and without avalanche generation illustrates the problems regarding unbounded solutions.

2. Delaunay grids, Voronoi diagrams, finite volume discretization. Let $\mathbf{x}_i^T = (x_{1,i}, x_{2,i}, \ldots, x_{N,i})$ denote the vector of the space coordinates of the vertex i, the $N \times N$ matrix

$$P_{l,k} = \begin{pmatrix} x_{1,k+1} - x_{1,k} & . & . & . & x_{1,k+N} - x_{1,k} \\ x_{2,k+1} - x_{2,k} & . & . & . & x_{2,k+N} - x_{2,k} \\ . & . & . & . & . \\ x_{N,k+1} - x_{N,k} & . & . & . & x_{N,k+N} - x_{N,k} \end{pmatrix}.$$

describes the lth N dimensional simplex $\mathbf{E}_l^N$ with respect to is local origin at vertex k (k is omitted often, $\mathbf{E}_l^1$ denotes an edge, short $\mathbf{e}_m$ or $\mathbf{e}_{ij}$). In a right handed coordinate system the vertices are numbered such, that $\det(P_l) > 0 \ \forall \ l$ holds. All vertices are assumed to be in general position to avoid the discussion of non uniqueness of Delaunay grids. Any Delaunay grid with vertices $\mathbf{x}_i$ in a degenerate case coinciding with one with vertices $\mathbf{y}_i = \mathbf{x}_i + \epsilon_i$ in general position for one special $\lim_{\epsilon_i \forall i} \to 0$ is equivalent to any other one regarding unique solutions of a finite volume discretization - non uniquely defined edges are associated with a zero geometric weight.
The domain is assumed to be constituted by subdomains $\mathbf{\Omega}_i$, each $\mathbf{\Omega}_i$ is associated with a single material.

$$\mathbf{\Omega} = \cup_i \mathbf{\Omega}_i = \cup_l \mathbf{E}_l^N.$$

DEFINITION 1. *A discretization by simplices $\mathbf{E}_i^N$ is called a Delaunay grid if the balls defined by the $N+1$ vertices of $\mathbf{E}_i^N \ \forall \ i$ do not contain any vertex $\mathbf{x}_k$, $\mathbf{x}_k \in \mathbf{E}_j^N$, $\mathbf{x}_k \notin \mathbf{E}_i^N$. [7].*

REMARK 1. *Let additionally each simplex $\mathbf{E}_l^N \in \bar{\mathbf{\Omega}}_i$ have its circum center in $\bar{\mathbf{\Omega}}_i$, then the discretization is called boundary conforming Delaunay. (This definition seems to be 'folklore' in some finite volume communities but is not so popular in grid generation circles – [8] gives an equivalent definition).*

DEFINITION 2. Let $V_i = \{\mathbf{x} \in I\!R^N : \|\mathbf{x} - \mathbf{x}_i\| < \|\mathbf{x} - \mathbf{x}_j\|, \forall \text{ vertices } \mathbf{x}_j \in \mathbf{\Omega}\}$ and $\partial V_i = \bar{V}_i \setminus V_i$. V_i is the Voronoi volume of vertex i and ∂V_i is the corresponding Voronoi surface.
The Voronoi volume element V_{ij} of the vertex i with respect to the simplex $\mathbf{E}_j^N$ is the intersection of the simplex $\mathbf{E}_j^N$ and the Voronoi volume V_i of vertex i.
V_i is constructed by the intersection of half spaces, hence convex. The requirement 'boundary conforming Delaunay mesh' results in simple properties of $V_i \cap \mathbf{\Omega}_j$ and each planar part of $\partial V_i \cap \partial \mathbf{\Omega}_j$. For vertex sets in general position ∂V_i related to each edge in the Delaunay grid has a positive measure - hence the Delaunay grid has minimal total edge length of all simplex tessellations of the given point set (especially in 2d acute meshes are boundary conforming Delaunay meshes).

The variant of finite volume schemes used here is characterized by 'integrating the equations over V_{ij}' and summation over j. It dates back at least to Macneal [9] (see [10], too). ∂V_{ij} is either a part of the Voronoi surface, hence orthogonal to an edge or part of $\partial \mathbf{E}_j^N$ - fluxes through these surfaces are compensated by neighbor simplices or are described by third kind boundary conditions,

$$\xi_1 u + \xi_2 \partial u/\partial \nu + \xi_3 = 0$$

with $\xi_1(x, u, \ldots) > 0$, $\xi_2(x, u, \ldots) > 0$, and ν the outer normal unit vector. The boundary conditions are integrated over the part of $\partial \mathbf{\Omega}_k \cap \partial V_{ij}$, where u is assumed to be spatially constant and approximated by u_i.
To start with, the discretization procedure is applied on the equation

$$-\nabla \cdot \epsilon \nabla u = f,$$

with a coefficient function ϵ constant in each subdomain ($\epsilon(x) = \epsilon_l, x \in \Omega_l$), and the approximation $\nabla u|_{\partial V_{i,k(i)}} \approx (\mathbf{u}_{k(i)} - \mathbf{u}_i)/|\mathbf{e}_{ik(i)}|$

$$\begin{aligned}\int_{V_{ij}} -\nabla \cdot \epsilon_l \nabla u \, dV &= -\epsilon_l \sum_{k(i)} \int_{\partial V_{i,k(i)}} \nabla u \cdot d\mathbf{S}_k \\ &\approx -\epsilon_l \sum_k \frac{\partial V_{i,k(i)}}{|\mathbf{e}_{i,k(i)}|}(u_k - u_i) + \mathrm{BI} = \epsilon_l [\gamma_{k(i)}] \tilde{G}_N(1,-1)\mathbf{u}|_{E_j^N} + \mathrm{BI}, \end{aligned} \tag{2.1}$$

where BI denotes boundary integrals due to the integration of the boundary conditions. The argument of $\tilde{G}(1,-1)$ should be understood as placeholder for special functions and is often omitted.

$$\int_{V_{ij}} f dV \approx V_{ij} f(x_i), \quad [V]_i = \sum_j V_{ij},$$

where $[\cdot]$ denotes a diagonal matrix. Integrals over Voronoi cells are replaced by local integrand value times volume. $\tilde{G}_N(1,-1)$ denotes a difference matrix, mapping from nodes to edges

$$(\tilde{G}^T \tilde{G})_{ii} > 0, \quad (\tilde{G}^T \tilde{G})_{i>j} < 0, \text{ and } \mathbf{1}^T \tilde{G}^T = \mathbf{0}^T. \tag{2.2}$$

$$\gamma_{k(i)} = \frac{\partial V_{i,k(i)}}{|\mathbf{e}_{i,k(i)}|}$$

denotes the elements of a diagonal matrix of geometric weights per simplex, $k(i)$ is a node connected to i by an edge $\mathbf{e}_{ik} \in E_j^N$. Summation over the nodes in the simplex j yields

$$\sum_{V_{ij} \in \mathbf{E}_j^N} \int_{V_{ij}} -\nabla \cdot \epsilon \nabla u dV \approx \epsilon \tilde{G}^T [\gamma] \tilde{G} \mathbf{u}|_{E_j^N} + \mathrm{BI}. \tag{2.3}$$

The explicit form of the boundary integrals is given by

$$\int_{E_j^{N-1} \cap V_i} -\epsilon \nabla u \cdot d\mathbf{S} \approx |E_j^{N-1} \cap V_i| \frac{\epsilon}{\xi_{2_j}} (\xi_{1_j} u_i + \xi_{3_j}),$$

where E_j^{N-1} denotes the $d-1$ dimensional simplex opposite to j. The boundary conditions yield non negative contributions to the diagonal entries and modify the right hand side. Dirichlet boundary conditions follow by $\xi_2 \to 0$ and can be directly eliminated or handled as properly chosen penalty with respect to the number representation used, resulting in fulfilled boundary conditions due to rounding. The notation $G^T[\cdot]G\mathbf{u}$ is used to indicate the global function including boundary conditions, too. The summation over all simplices and its reordering over edges, nodes, etc. is not indicated explicitly as long as the global or local meaning follows from the context.
Due to the the local current conservation with respect to each Voronoi volume V_i at node i (2.1) it is possible to introduce discrete test functions in complete similarity to integration by parts (compare 2.3) to evaluate contact currents. Definition of the test functions by the related adjoint problem results in first order error cancellation [11], compare Table 4.1. Accordingly a 'weak discrete maximum principle' holds as long as the Voronoi faces related to each edge and subdomain fulfill

$$\sum_{E_j^N \ni \mathbf{e}_{ik}, E_j^N \in \Omega_i} \partial V_{ik} \geq 0. \tag{2.4}$$

This is exactly the requirement fulfilled by a 'boundary conforming Delaunay grid'. Summation over all simplices yields for connected grids an irreducible, weakly diagonally dominant matrix due to the third kind boundary conditions with some $\xi_1\xi_2 > 0$. This matrix has a bounded, non negative inverse – due to maximum principle or Perron-Frobenius theory (see [10]).
Hence Voronoi surface (short 'edge') related, positivity preserving averaging schemes of more general coefficient functions, $\bar{\epsilon}_{e_{ik}} = \sum_{E_j^N \ni \mathbf{e}_{ik}, E_j^N \in \Omega_i} \overline{\epsilon(x, u, |\nabla u|)}$ resulting in $\sum_{E_j^N \ni \mathbf{e}_{ik}, E_j^N \in \Omega_i} \bar{\epsilon}_{e_{ik}} \partial V_{ik} \geq 0$, preserve the maximum principle, hence the existence of a bounded, non negative inverse.
It is convenient to introduce $V_{ij} < 0$, $\partial V_{ij} < 0$ to establish local per element quantities. This results in formally complex 'gradient' matrices $G = \sqrt{[\gamma]}\tilde{G}(1,-1)$ for simplices not containing their circum center (functions and relations like $\sqrt{[x]}$, $\mathbf{x} < \mathbf{y}$ should be understood in a per matrix element meaning). Summation rules of usual expressions avoid any use of the complex quantities. The price paid is: in general $\mathbf{u}^T|_{E_j^N} G^T G \mathbf{u}|_{E_j^N}$ does not introduce a discrete gradient seminorm on one simplex only. A convenient way out in case of parameter evaluations is to take advantage of the related finite element expression $||\nabla u||^2|_{E_j^N} := |E_j^N| \mathbf{u}^T P_j^{-T} P_j^{-1} \mathbf{u}$ and to use these gradients in edge related, positivity preserving averaging schemes.

3. Scharfetter-Gummel-scheme and bounded discrete solutions. With these prerequisites bounds for the discrete steady state solutions on a fixed, boundary conforming Delaunay grid can be derived by closely following the analytic results. Application of the procedure on the continuity equations in so called Slotboom variables $u := e^{-\phi_n}$, $v := e^{\phi_p}$ yields by solving a two point boundary problem along each edge for piecewise linear $w(x)$ (first integration yields $\bar{\mu} e^{w} (e^{-\phi_n})' = const$, the second one results in the used relation between w_l, $\phi_{n,l}$, $l = i, k(i)$ for edge $\mathbf{e}_{i,k(i)}$, where $\bar{w} := (w_i + w_{k(i)})/2$, $\mathrm{sh}(s) := \sinh(s)/s$ is related to the Bernoulli function $b(2s) = e^{-s}/\mathrm{sh}(s) = 2s/(e^{-2s}-1)$, $\mathrm{sh}(s) = \mathrm{sh}(-s) \geq 1$, while *const* has the meaning of a current and is substituted in Gauss's theorem). The variation of μ_i is assumed to be small compared with that of $w(x)$, hence μ is averaged, like ϵ, on the edge related part of the Voronoi surface and its intersection with each subdomain to preserve (2.4). The average is denoted by $\bar{\mu}$. It is the well known Scharfetter-Gummel scheme [12] in

symmetric form, the discrete variables are transformed by positive diagonal matrices. The discrete problem reads:

$$G^T\epsilon G\mathbf{w} = [V]\mathbf{g}(\mathbf{C},\mathbf{n},\mathbf{p}),\ \mathbf{g} = \mathbf{C} - \mathbf{n} + \mathbf{p},\ \Omega,\ \mathbf{n} = [e^w]\mathbf{u},\ \mathbf{p} = [e^{-w}]\mathbf{v}, \tag{3.1}$$

$$A_{S_n}(\mu_n,\mathbf{w})\mathbf{e}^{-\phi_n} = G^T[\bar{\mu}_n e^{\bar{w}}/\mathrm{sh}(\tilde{G}\mathbf{w}/2)]G\mathbf{u} = [V][r(\mathbf{x},\mathbf{n},\mathbf{p})](\mathbf{1} - [v]\mathbf{u}), \tag{3.2}$$

$$A_{S_p}(\mu_p,-\mathbf{w})\mathbf{e}^{\phi_p} = G^T[\bar{\mu}_p e^{-\bar{w}}/\mathrm{sh}(\tilde{G}\mathbf{w}/2)]G\mathbf{v} = [V][r(\mathbf{x},\mathbf{n},\mathbf{p})](\mathbf{1} - [u]\mathbf{v}). \tag{3.3}$$

Here $r > 0$ denotes a differentiable function, for further details and dissipativity, which may be the strongest constraint for deriving averages, see [13].

On insulating boundary parts the normal derivatives of the quasi-Fermi-potentials vanish $\partial\phi_k/\partial\nu = 0$ ($k = n, p$, ν outer normal). The boundary conditions at Ohmic contacts are (due to charge neutrality, infinite recombination velocity, and infinite conductivity of a metallic contact)

$$w|_{\Gamma_{D_k}} = w_k + w_{b,k},\ e^{w_{b,k}} - e^{-w_{b,k}} = C|_{\Gamma_{D_k}}, u|_{\Gamma_{D_k}} = e^{-\phi_{n,k}},\ v|_{\Gamma_{D_k}} = e^{\phi_{p,k}}, \tag{3.4}$$

where $w_k = \phi_{n,k} = \phi_{p,k}$ is the 'applied potential', zero in thermodynamic equilibrium, while $w_{b,k}$ is the 'built-in voltage'. These boundary conditions fix one arbitrary constant in ϕ_n and ϕ_p – due to $np = 1$, hence the thermodynamic equilibrium solution is ($\mathbf{w}^*$, $\mathbf{u}^* = \mathbf{1}$, $\mathbf{v}^* = \mathbf{1}$) and $\mathbf{w}^*$ solution of (3.1) with $\mathbf{u} = \mathbf{u}^*$, $\mathbf{v} = \mathbf{v}^*$. If the doping concentration C is not constant on a conducting boundary section Γ_{D_k}, $w_{b,k}$ should be understood as the constant on Γ_{D_k} electrostatic potential difference, resulting in zero electron and hole current at that contact. Third kind boundary conditions (Gate and Schottky contacts) having the proper sign relations can be handled in a similar way - here they are omitted.

PROPOSITION 1. *Suppose $-\infty < \check{w}_0 \le w \le \hat{w}_0 < \infty$. A_{S_n}, A_{S_p} are weakly diagonally dominant matrices, hence have bounded positive inverses due to the positive Dirichlet boundary measure.*

PROOF: $\bar{\mu}(E_j^N, \mathbf{e}_{i,k(i)}) = \bar{\mu}(E_{j'}^N, \mathbf{e}_{i,k(i)}) > 0\ \forall\ E_m^N \in \Omega_l, m = j, j',$ and $\mathbf{e}_{i,k(i)} \in E_m^N$ holds due to the assumed average. Hence $0 < [\bar{\mu}e^{\bar{w}}/\mathrm{sh}(\tilde{G}\mathbf{w})] < \infty$ holds, the sign pattern and the sum relations (2.2) are not changed. □

Assume

$$\check{u} \le u_i^0 \le \hat{u},\ \check{v} \le v_i^0 \le \hat{v}\ \forall\ x_i \in \bar{\Omega}. \tag{3.5}$$

The right hand side of the discrete Poisson equation $g_i(C_i, n_i, p_i)$ is with respect to w_i a strictly monotone mapping of $\mathbb{R}$ onto $\mathbb{R}\ \forall i$. Let $\check{C} = \min(C(x))$ and $\hat{C} = \max(C(x))$ denote the minimum and maximum of the doping concentration. Hence the solution $\check{w}_i$ of $\mathbf{g}(\check{w}_i) = 0$ at any vertex $x_i \in \Omega$ fulfills the bounds

$$e^{\check{w}} := \frac{\check{C}}{2\hat{u}} + \sqrt{\frac{\check{C}^2}{4\hat{u}^2} + \frac{\check{v}}{\hat{u}}} \le e^{\check{w}_i} \le \frac{\hat{C}}{2\check{u}} + \sqrt{\frac{\hat{C}^2}{4\check{u}^2} + \frac{\hat{v}}{\check{u}}} =: e^{\hat{w}}. \tag{3.6}$$

PROPOSITION 2. *The discrete electrostatic potential $\mathbf{w}^0$, the unique solution of (3.1) with $\mathbf{w}$ replaced by $\mathbf{w}^0$, $\mathbf{u}$, $\mathbf{v}$ by $\mathbf{u}^0$, $\mathbf{v}^0$, and fulfilled assumption (3.5) can be estimated by*

$$\check{w} := \min(w|_{\Gamma_D}, \check{w}) \le w_i^0 \le \max(w|_{\Gamma_D}, \hat{w}) =: \hat{w}. \tag{3.7}$$

PROOF: Suppose $w_j^0 > \acute{w}$. Testing (3.1) with the positive part $(\mathbf{w}^0 - \acute{w})^+$ yields

$$(\mathbf{w}^0 - \acute{w})^{+T} G^T \epsilon G \mathbf{w}^0 - (\mathbf{w}^0 - \acute{w})^{+T} [V] \mathbf{g}(\mathbf{C}, \mathbf{w}^0, \mathbf{u}^0, \mathbf{v}^0) = 0.$$

Because $\mathrm{sign} G(\mathbf{w}^0 - \acute{w})^+ = \mathrm{sign} G\mathbf{w}^0$ if $G(\mathbf{w}^0 - \acute{w})^+ \neq 0$ is true, $g(\hat{C}, \hat{w}, \check{u}, \hat{v}) = 0$ holds by construction (3.1, 3.6), $(\mathbf{w}^0 - \acute{w})^{+T} G^T \epsilon G \mathbf{w}^0 > 0$ and $(\mathbf{w}^0 - \acute{w})^{+T} [V] \mathbf{g}(\mathbf{C}, \mathbf{w}^0, \mathbf{u}^0, \mathbf{v}^0)$ ≤ 0 result in a contradiction. Similarly follows the lower bound by testing with the negative part $(\mathbf{w}^0 - \grave{w})^-$. The mapping with respect $\mathbf{w}^0$ is continuous, differentiable, and bounded and maps the convex domain $\grave{w} \leq w_i^0 \leq \acute{w}$ onto itself. The linear problem with $\mathbf{g} = \mathbf{0}$ has a unique solution ($G^T \epsilon G$ is weakly diagonally dominant) and embedding with respect to $\mathbf{g}$ does not change the degree. Uniqueness follows directly from maximum principle: let $\mathbf{w}_1^0$, $\mathbf{w}_2^0$ to be solutions of (3.1), assume $(\mathbf{w}_1^0 - \mathbf{w}_2^0)^+ > 0$ for at least one $x_i \in \Omega$, testing

$$(\mathbf{w}_1^0 - \mathbf{w}_2^0)^{+T} G^T \epsilon G (\mathbf{w}_1^0 - \mathbf{w}_2^0) - (\mathbf{w}_1^0 - \mathbf{w}_2^0)^{+T} [V] (\mathbf{g}(\mathbf{w}_1^0) - \mathbf{g}(\mathbf{w}_2^0)) = 0,$$

and using the monotonicity of g with respect to w_i yields a contradiction. □

PROPOSITION 3. *Let* $\mathbf{w}^1$ *be a solution of*

$$G^T \epsilon G \mathbf{w}^1 = [V] \mathbf{g}(\mathbf{C}, \mathbf{w}^1, \mathbf{u}^0, \mathbf{v}^0), \tag{3.8}$$

where $\mathbf{u}^0$, $\mathbf{v}^0$ *respect the bounds (3.5) and suppose* $\mathbf{u}^1$, $\mathbf{v}^1$ *to be solutions of the decoupled continuity equations*

$$A_S(\mu_n, \mathbf{w}^1)\mathbf{u}^1 = [V] r(\mathbf{x}, e^{\mathbf{w}^1}\mathbf{u}^0, e^{-\mathbf{w}^1}\mathbf{v}^0)(\mathbf{1} - [v^0]\mathbf{u}^1), \tag{3.9}$$

$$A_S(\mu_p, -\mathbf{w}^1)\mathbf{v}^1 = [V] r(\mathbf{x}, e^{\mathbf{w}^1}\mathbf{u}^0, e^{-\mathbf{w}^1}\mathbf{v}^0)(\mathbf{1} - [u^0]\mathbf{v}^1). \tag{3.10}$$

Assume for some sufficiently large w^+,
$\max(w|_{\Gamma_D}) - \min(w|_{\Gamma_D}) \leq w^+ < \infty$, *that*

$$e^{-w^+} \leq \mathbf{u}^0, \;\; \mathbf{v}^0 \leq e^{w^+}$$

is true. Then e^{w^-}, e^{w^+} *is an lower, upper solution respectively for equations (3.9, 3.10).*

PROOF: Assuming $\mathbf{u}^1 > e^{w^+}$ for at least one $x_i \in \Omega$ and testing (3.9) with $(\mathbf{u}^1 - e^{w^+})^{+T}$ yields $(\mathbf{u}^1 - e^{w^+})^{+T} A_S(\mu_n, \mathbf{w}^1)\mathbf{u}^1 > 0$ independently of μ_n, $\mathbf{w}^1$. On the other hand $(\mathbf{1} - [v^0]\mathbf{e}^{w^+}) \leq \mathbf{0}$, and $[r(\mathbf{x}, e^{\mathbf{w}^1}\mathbf{u}^0, e^{-\mathbf{w}^1}\mathbf{v}^0)] > 0$ hold, hence $\mathbf{u} \leq e^{w^+}$ follows, and so do the other bounds. □

REMARK 2. *Choosing in (3.5)* $\check{u}$, $\hat{u}$, $\check{v}$, $\hat{v}$ *accordingly* $\underline{u} = \underline{v} = e^{-w^+}$, $\overline{u} = \overline{v} = e^{w^+}$ *yields*

$$\underline{u} \leq \mathbf{u} \leq \overline{u}, \tag{3.11}$$

$$\underline{v} \leq \mathbf{v} \leq \overline{v}, \tag{3.12}$$

and with (3.7)

$$\underline{w} = \min(w|_{\Gamma_D}, \ln((\check{C} + \sqrt{\check{C}^2 + 4})/2) - w^+) \leq w \tag{3.13}$$

$$w \leq \max(w|_{\Gamma_D}, \ln((\hat{C} + \sqrt{\hat{C}^2 + 4})/2) + w^+) = \overline{w}. \tag{3.14}$$

These are the final bounds because Proposition 3 is true with (3.11, 3.12, 3.13, 3.14), too.
The bounds are identical with the analytic ones (compare [4]).
The summary of the results is:

THEOREM 3.1. *On any connected, boundary conforming Delaunay grid with n vertices, the problem (3.1, 3.2, 3.3) with positive Dirichlet boundary measure has at least one solution. It fulfills the bounds (3.11, 3.12, 3.13,3.14).*
PROOF: The established bounds form a convex set in $\mathbb{R}^{3n}$ and the two step mapping (Proposition 2, 3.9, 3.10) is continuous, differentiable, and maps the convex set onto itself, hence Brouwer's fixed point theorem guarantees the existence of at least one fixed point. □

Uniqueness for small applied voltages follows by showing the existence of a bounded inverse of the Jacobian of the linearization of (3.1, 3.2, 3.3) (nonlinear boundary conditions are linearized, too) at equilibrium. Due to the smooth dependence of all functions on all variables involved in the discretization it is invertible in a sufficiently small neighborhood of the equilibrium. The linearization at an approximate solution $(\tilde{\mathbf{u}}, \tilde{\mathbf{v}}, \tilde{\mathbf{w}})$, $\tilde{\mathbf{u}} + \delta\mathbf{u} \approx \mathbf{u}$, $\tilde{\mathbf{v}} + \delta\mathbf{v} \approx \mathbf{v}$, $\tilde{\mathbf{w}} + \delta\mathbf{w} \approx \mathbf{w}$, $\tilde{\mathbf{n}} = [e^{\tilde{w}}]\tilde{\mathbf{u}}$, $\tilde{\mathbf{p}} = [e^{-\tilde{w}}]\tilde{\mathbf{v}}$ reads:

$$(G^T \epsilon G + [V][\tilde{n} + \tilde{p}])\delta\mathbf{w} + [Ve^{\bar{w}}]\delta\mathbf{u} - [Ve^{-\bar{w}}]\delta\mathbf{v} = -\mathbf{f}_1,$$

$$(G^T Y_n - [V](I - [\tilde{v}][\tilde{u}])\frac{\partial r}{\partial \tilde{w}})\delta\mathbf{w} + (A_{S_n}(\mu_n, \tilde{\mathbf{w}}) - [V][d_n])\delta\mathbf{u} - [V][d_p]\delta\mathbf{v} = -\mathbf{f}_2,$$

$$(G^T Y_p - [V](I - [\tilde{v}][\tilde{u}])\frac{\partial r}{\partial \tilde{w}})\delta\mathbf{w} + [V][d_n]\delta\mathbf{u} + (A_{S_p}(\mu_p, -\tilde{\mathbf{w}}) - [V][d_p])\delta\mathbf{v} = -\mathbf{f}_3.$$

$\mathbf{f}_i$ are the function values, evaluated at an iterate or a guess with the boundary conditions of ($\mathbf{u}$, $\mathbf{v}$, $\mathbf{w}$) included by proper changes of ξ_3 at the related parts of the boundary and with or without homogenization and continuation by smooth functions to $x_i \in \Omega$ – the first iterate fulfills the boundary conditions used here in any case.
$[d_j]$, Y_j, $j = n, p$ are defined by

$$[d_n] = [\frac{\partial r}{\partial \tilde{u}}](I - [\tilde{u}\tilde{v}]) - [r][\tilde{v}],$$

$$[d_p] = [\frac{\partial r}{\partial \tilde{v}}](I - [\tilde{u}\tilde{v}]) - [r][\tilde{u}],$$

$$Y_n = [\tilde{G}\tilde{\mathbf{u}}]\frac{\partial}{\partial \tilde{w}}[\bar{\mu}_n e^{\bar{w}}/\mathrm{sh}(\tilde{G}\tilde{\mathbf{w}}/2)],$$

$$Y_p = [\tilde{G}\tilde{\mathbf{v}}]\frac{\partial}{\partial \tilde{w}}[\bar{\mu}_p e^{-\bar{w}}/\mathrm{sh}(\tilde{G}\tilde{\mathbf{w}}/2)].$$

Choosing the thermodynamic equilibrium solution as the approximate one, the problem simplifies due to $G\tilde{\mathbf{u}} = G\tilde{\mathbf{v}} = G\mathbf{1} = \mathbf{0}$, $[\tilde{u}\tilde{v}] = I$, and $[d_n] = [d_p] = -[r]$, hence it is sufficient to show the existence of a bounded inverse for the linearized continuity equations.

PROPOSITION 4. *Suppose* $[d_j] < 0$, $\forall x_i \in \Omega$, *and* $[d_j]|_{\Gamma_D} = 0, \quad [D_j] = -[V][d_j]$, $j = n, p$. *Then the Schur complement*

$$S = A_{S_p} + [D_p] - [D_n](A_{S_n} + [D_n])^{-1}[D_p]$$

of

$$\tilde{A} = \begin{pmatrix} A_{S_n} + [D_n] & [D_p] \\ [D_n] & A_{S_p} + [D_p] \end{pmatrix}, \tag{3.15}$$

is a weakly diagonally dominant matrix with $S_{ii} > 0$, $S_{ij} \leq 0$ *and* $i \neq j$.
PROOF: Solutions $\mathbf{z}$ with $\mathbf{z}|_{\Gamma_D} = 0$

$$(A_{S_n} + [D_n])\mathbf{z} = \mathbf{e}_i, \quad \mathbf{e}_i = 1 \text{ at one } x_i \in \Omega$$

fulfill $0 \leq \mathbf{z}$ and $\mathbf{D}_n^T\mathbf{z} < 1$ ($\mathbf{1}^T[\text{sign}D_n]A_{S_n} = \mathbf{y} \geq \mathbf{0}$, and $y_i > 0$ $\forall x_i \in \Omega$ and next neighbors of Γ_D). Hence for the column sum holds $\mathbf{1}^T(I - [D_n](A_{S_n} + [D_n])^{-1})[D_p] > 0$, the off-diagonal elements fulfill $\mathbf{e}_i^T(I - [D_n](A_{S_n} + [D_n])^{-1})[D_p]\mathbf{e}_j < 0$, $i \neq j$ $\forall i, j \in \Omega$, and 0 on Γ_D, hence sign pattern and column sum relation are fulfilled for S, too. □
With $[D_n] = [D_p] = [V][r]$ the matrix S is symmetric positive definite.

4. Example. To give an example a modified CoolMOS like device is depleted by an embedding process with respect to the applied voltage. An introduction to the principles of operation of CoolMOS devices can be found for instance in [14]. The very basic idea is to chose doping levels and the geometry in such a way, that the N and the P doped regions are depleted together starting from the folded *pn*-junction in the off-state and to use a MOSFET to control the on-state in such a way, that the majority carriers don't pass any *pn*-junction. The folded *pn*-junction is crucial for the maximal switching voltage reached, which is limited by avalanche generation. 1, 4, and 16 elementary cells are computed exactly within the framework given above and with the extension of an unbounded avalanche generation term. The avalanche generation results in a blow up in finite time in the experimental setup, too. The static embedding process is stopped at current and avalanche generation levels, that clearly indicate: the major part of the current results from avalanche generation.

The modification of a CoolMOS device consists in a more complicated geometry: an infinite hexagonal array s formed by different intersecting cylinders defining the N, N^+, P, P^+ regions and a SiO_2 domain, which is not present in a typical CoolMOS. This second material introduces edge singularities, which are influencing the avalanche generation directly, and allows for the formation of boundary layers, which move in dependence of the applied voltage in tangential direction along the $Si - SiO_2$ interface. These boundary layers influence the charge distribution, hence the conductivity and the avalanche generation. They are used to add complexity to the numerical solution and to illustrate the fact: these features are hardly to resolve by the grid with smallness assumptions for the discretization like $|\tilde{G}\mathbf{s}| < c << 1$ or $\exp(c) < 1$, $\mathbf{s} = \mathbf{w}, \phi_\mathbf{n}, \phi_\mathbf{p}$, hence discretization schemes with proven unconditional stability are essential for solving these problems numerically.

The computation of more than one elementary cell is of interest, because
a) any real world device is finite in size and the perturbations of the infinite grid introduced at the insulating structures forming the device boundary are often critical,
b) symmetric structures allow for numerical consistency tests - in the avalanche case by systematically approaching a singular problem.

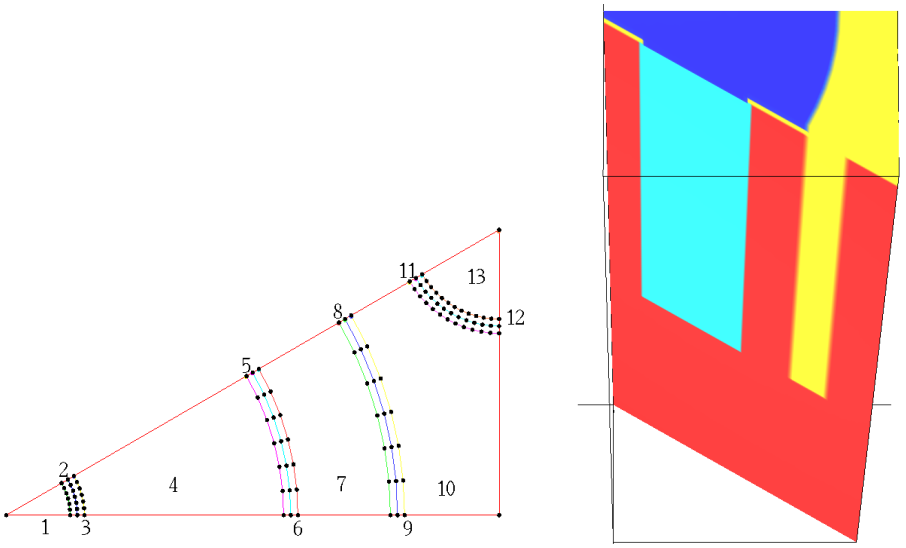

FIG. 4.1. *Top view of one elementary cell, the numbers indicate different regions (left). Material distribution in the elementary cell: blue P^+ (carries the TOP contact), light blue P, yellow SiO_2, red N (the lower triangle forms the BOTTOM contact).*

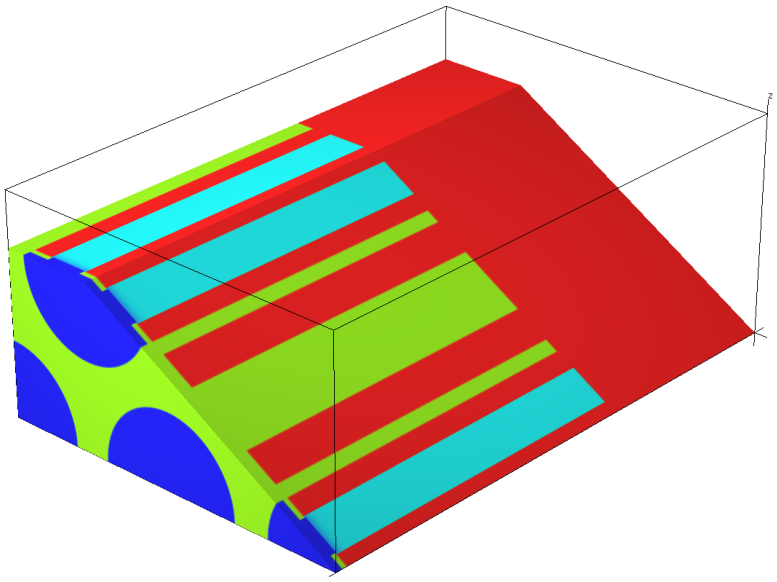

FIG. 4.2. *Material distribution in 16 elementary cells, the top most one is cut of in the figure.*

Short description of the numerical solution methods: The basic algorithm is an approximate Newton's method with an exact Jacobian. Different preconditioning methods are combined and used in dependence of the state and user settings. CGS [15] is used to combine the solutions of scalar equations to one solution of the Newton linearized system. Details will be published elsewhere, the essential step is to solve very ill conditioned equations close to those of diffusion convection type in divergence form. PARDISO (see [16] for instance) is used presently – it causes the practical size

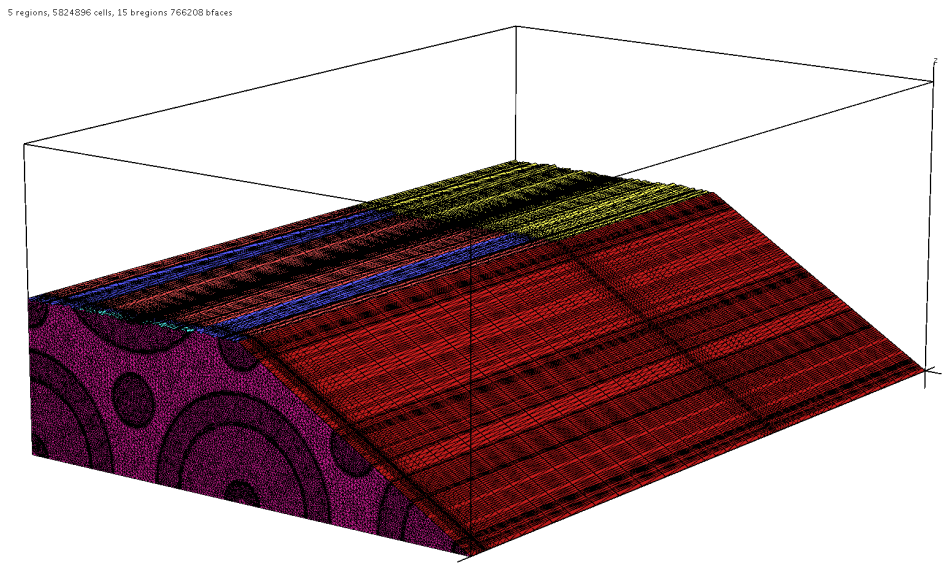

FIG. 4.3. *Typical grid, 1006791 nodes, 5824896 tetrahedra, shown is the surface and a cut (z = const).*

limitations but solves the equations with the necessary reliability and the algorithms used reach a large number of solutions per factorization. The algorithms are sufficient to differentiate the sensitivity to avalanche generation between different design modifications without introducing an additional grid size dependence on top of that one due to solving scalar degenerate elliptic problems in three space dimensions. This range is roughly described by: the integrated generation rate of Schockley-Read-Hall type is above that of avalanche processes (the Okuto-Crowell-model was used here [17]). This is of course not any more the case close to the avalanche breakdown.

The following figures and Table 4.1 should give an impression regarding the cases without avalanche (computed with numerical control parameters identical in all cases - hence defined by those including avalanche). The cases with avalanche are characterized essentially by how far one wants to follow the blow up along the nearly vertical tangent (see Figure 4.5). The stopping criteria are: $||\delta \mathbf{w}||_\infty + ||\delta \phi_\mathbf{n}||_\infty + ||\delta \phi_\mathbf{p}||_\infty \leq 0.015 U_T$ for Newton's method and an error reduction of 10^{-4} for CGS. In cases without avalanche the latter can be relaxed and controlled depending on the non linear iteration.

The three cases are recomputed with avalanche generation and an avalanche generation specific preconditioner, which does not remove the singularity of the problem but allows to reach significant levels of avalanche generation using the same solution techniques. The following Figures 4.7, 4.8 show the depleted state at 361.494V without avalanche generation and details of solutions.

A comparison of the numerically computed results of the different geometrical cases shows nearly identical results, a small symmetry breaking effect is present at larger avalanche generation levels. It results in a small but almost equal reduction of the avalanche generation levels for 4 and 16 elementary cells (see Fig. 4.5). The number of CGS iterations increases with the diminishing distance to singularity and

cells	nodes	tot. # of emb. steps	rejected emb. steps	tot. # of Newton it.	av. CGS it. per Newton it.
1	66462	306	18	1979	6.165
4	256386	315	20	2006	6.564
16	1006791	305	18	1961	6.151

av. # factoriz. per Newton it.	tot. # scalar 3d problems solved	av. solved lin. sys. per factorization	memory used / MB	max. rel. err. current balance
3*0.3497	122010	58.77	272.5	10^{-13}
3*0.3601	131680	70.91	1072.4	$2 \cdot 10^{-13}$
3*0.3187	120620	64.33	4357.6	$4 \cdot 10^{-12}$

TABLE 4.1

Some quantities characterizing the algorithms used to solve 3 depletion problems (CoolMOS without avalanche, BOTTOM $0V \rightarrow 400V$, memory used: memory used without PARDISO).

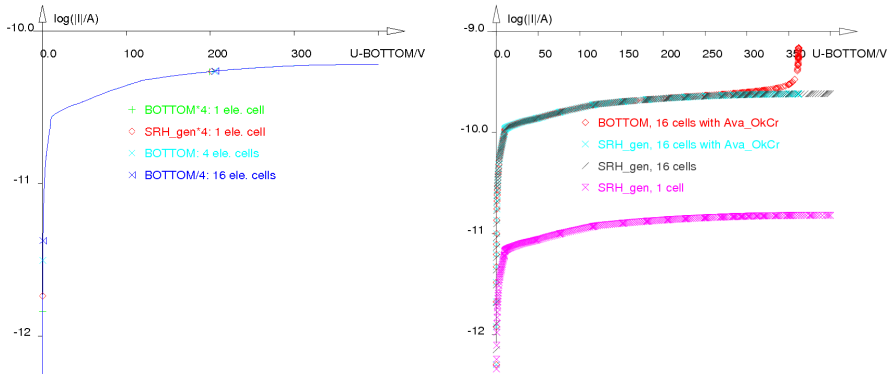

FIG. 4.4. *Depletion of 1, 4, 16 elementary cells without avalanche generation, scaled (by 4 respectively 1/4) contact currents (left, SRH stands for the integrated Schockley-Read-Hall recombination/generation rate), the embedding process depends very weakly on the number of elementary cells and the avalanche generation up to 357V (shown are all computed points, right).*

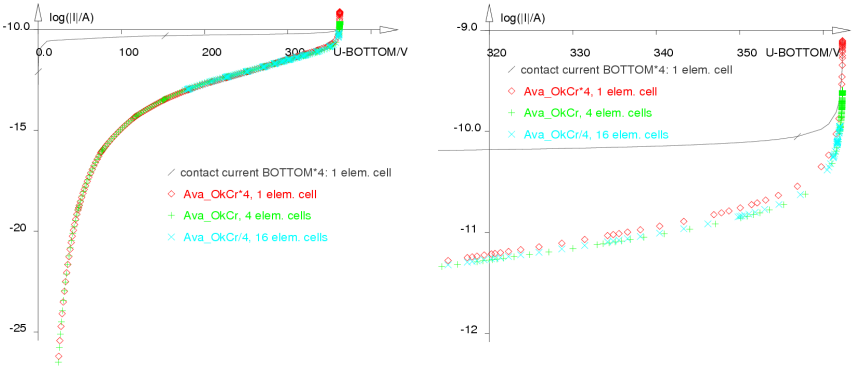

FIG. 4.5. *Avalanche breakdown 'CoolMOS', 1, 4, and 16 elementary cells, detail right, shown is the logarithm of the avalanche generation rate (normalized to 1A) for each embedding step, step size limitations at low avalanche generation levels are often due to the tangential movement of the boundary layers along the $Si - SiO_2$ interfaces (compare Figure 4.7).*

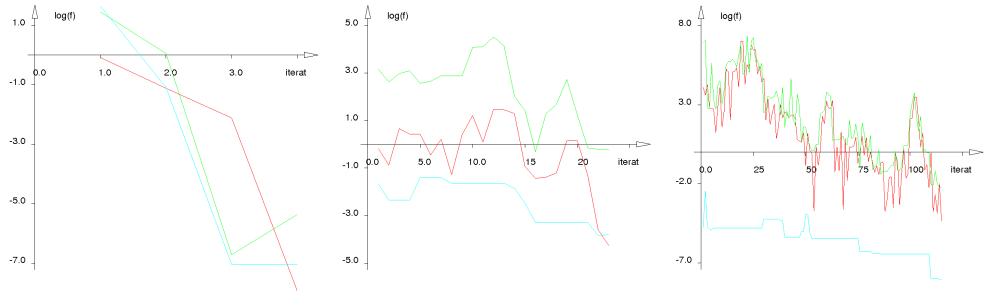

FIG. 4.6. *Avalanche breakdown 'CoolMOS', 16 elementary cells, the typical increase of CGS iterations with increasing avalanche generation, applied voltages 179V, 357V, 361.5V (left to right); logarithm of the* $||\cdot||_\infty$ *of the preconditioned residuum (green), true residuum (blue), update (red).*

the number of elementary cells. The symmetry breaking effect could be a combination of at least any of the following reasons:
a) the grids fulfill symmetry conditions with respect to the vertices but a few edges are flipped to construct a consistently extended grid, hence gradients are computed on tetrahedra that fulfill symmetry conditions only with exceptions;
b) limited precision in solving the linear and nonlinear systems of equations (precision limits are close: recomputation of the 1 elementary cell case on different computer architectures with different numbers of processors shows deviations of the same size);
c) filamentation effects due to the physical model can not be excluded, but are not seen as the favorite reason.
Without avalanche generation and its amplification effects the deviations in the solutions and related integrals like contact currents (Figure 4.4) are negligible for the three systematically extended test cases. Here the point symmetry is sufficient to construct completely symmetric extensions.

REFERENCES

[1] M. S. Mock. *Analysis of Mathematical Models of Semiconductor Devices*. Boole Press, Dublin, 1983.
[2] J. W. Jerome. Consistency of Semiconductor Modeling: An Existence/Stability Analysis for the Stationary Van Roosbrook System. *SIAM J. Appl. Math.*, 45:565–590, 1985.
[3] H. Gajewski. On existence, uniqueness and asymptotic behavior of solutions of the basic equations for carrier transport in semiconductors. *Z. Angew. Math. Mech.*, 65:101–108, 1985.
[4] P. A. Markowich. *The Stationary Semiconductor Device Equations*. Springer, Wien, 1986.
[5] H. Gajewski and K. Gröger. Initial-boundary value problems modelling heterogeneous semiconductor devices. In *Surveys on Analysis, Geometry and Mathematical Physics*, volume 117 of *Teubner-Texte Math.*, pages 4–53. Teubner, Leipzig, 1990.
[6] M. Zlamal. Finite Element Solution of the Fundamental Equations of Semiconductor Devices I. Report, Department of Math., Technical University Brünn, CSSR, 1984.
[7] B. Delaunay. Sur La Sphére Vide. *Izvestia Akademii Nauk SSSR. Otd. Matem. i Estestv. Nauk*, 7:793 – 800, 1934.
[8] P. Fleischmann. Mesh Generation for Technology CAD in Three Dimensions. *Dissertation*, Technische Universität, Wien, 1999.
[9] R. H. Macneal. An asymmetrical finite difference network. *Quart. Math. Appl.*, 11:295–310, 1953.
[10] R. S. Varga. Matrix Iterative Analysis. Prentice-Hall, 1962. Englewood Cliffs, N. J.
[11] K. Gärtner. Depfet sensors, a test case to study 3d effects. *Journal of Computational Electronics*, 6:275–278, 2007.
[12] D. L. Scharfetter and H. K. Gummel. Large–signal analysis of a silicon read diode oscillator.

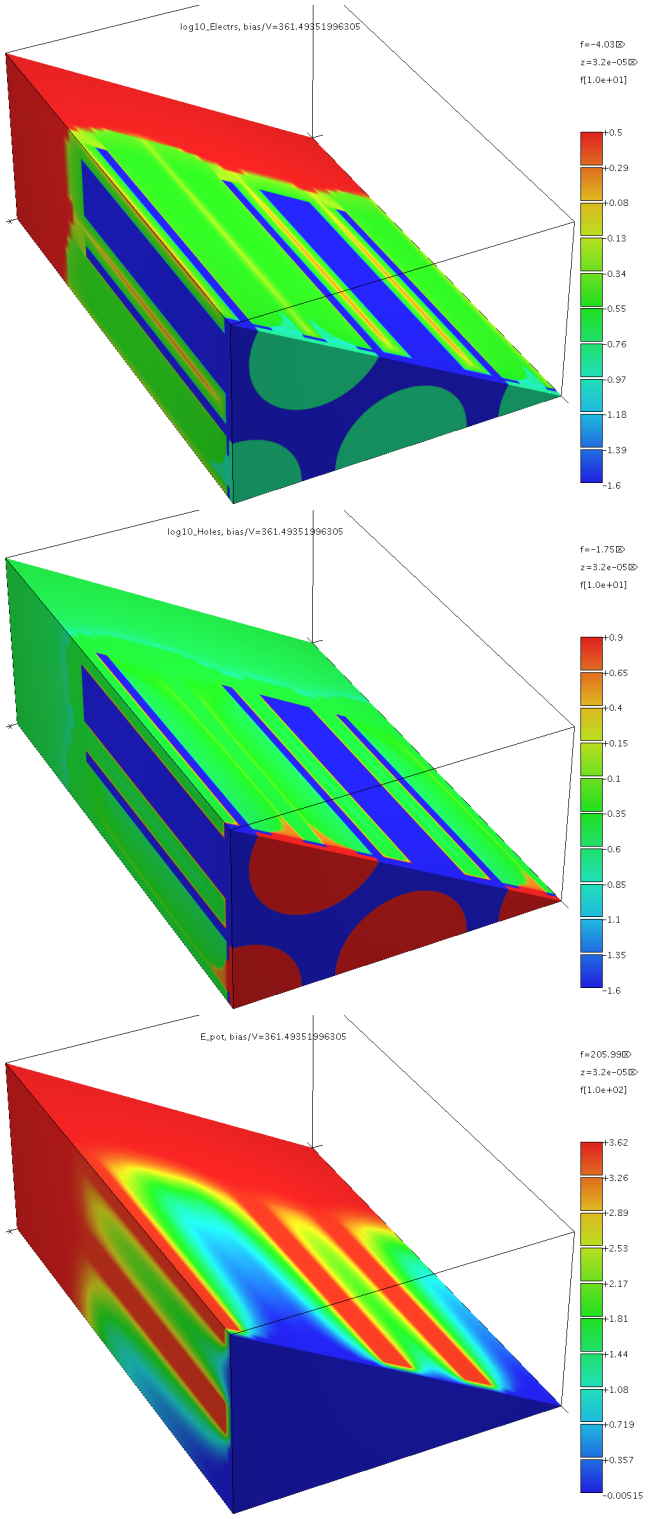

FIG. 4.7. *Global view on the solution (no avalanche generation, 361.494V):*

logarithm of the electron density,

logarithm of the hole density,

electrostatic potential in V; (electrons: red large density 5, turquoise small -12, blue SiO_2, holes: red large density 9, turquoise small -8, blue SiO_2, electrostatic potential: red 362V, blue -0.5V).

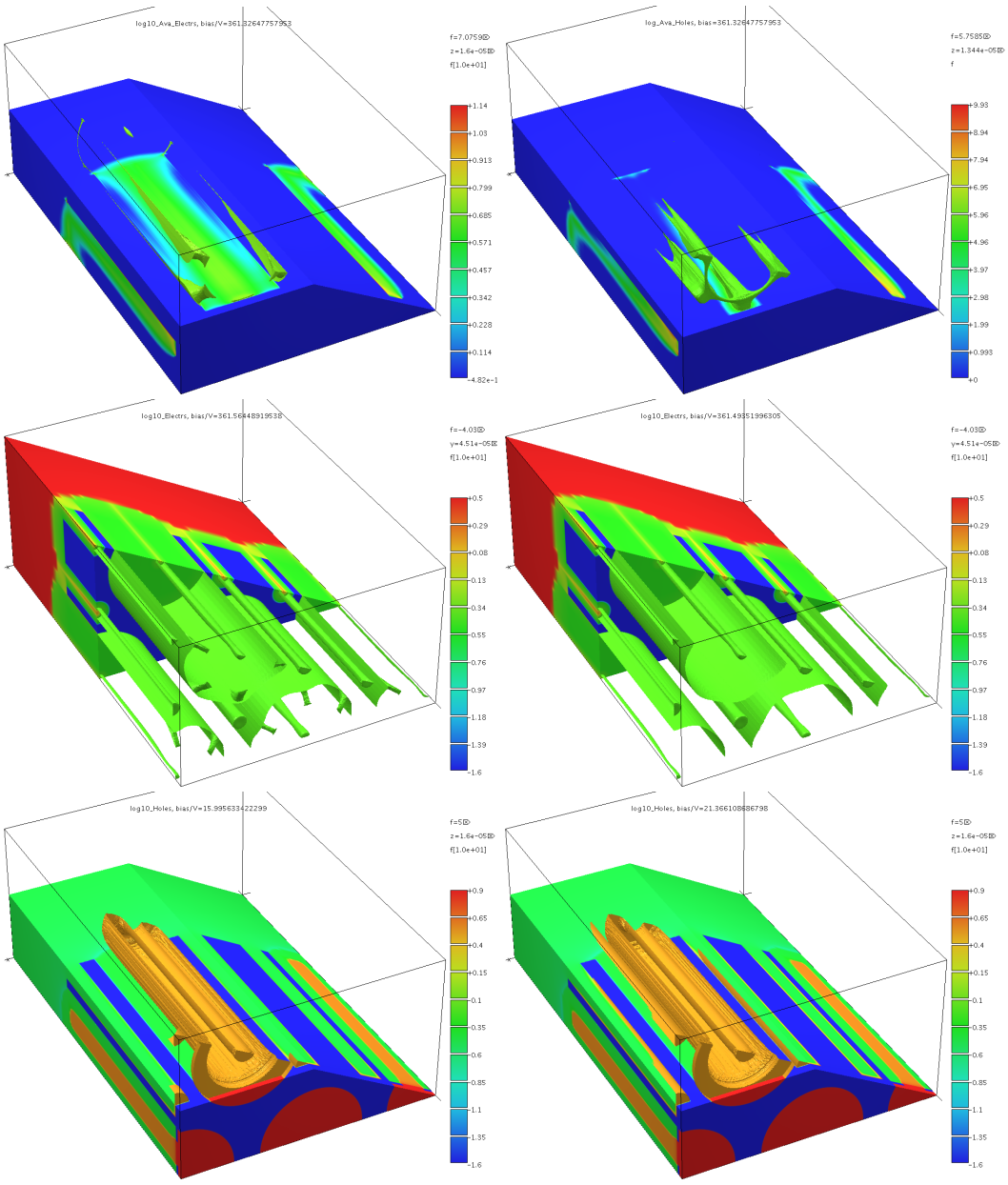

FIG. 4.8. *Solution details (top to bottom): avalanche generation influences the carrier density distributions, logarithm of the avalanche generation rate due to electrons (left), due to holes (right); logarithm of the electron density with one isosurface showing deformations due to the avalanche generated electrons (left), without avalanche generation (right); moving boundary layers at the* $Si - SiO_2$ *interface, logarithm of the hole density, 16.0V (left), 21.37V (right); 3d graphics by* `gltools`.

IEEE Trans. Electr. Dev., 16:64 – 77, 1969.

[13] H. Gajewski and K. Gärtner. On the discretization of van Roosbroeck's equations with magnetic field. *Z. Angew. Math. Mech.*, 76:247–264, 1996.

[14] M. Schmitt. Optimierung dynamischer elektrischer Eigenschaften von Kompensationsbauelementen. volume 17 of *Selected Topics of Electronics and Micromechatronics*. Schaker, Aachen, 2005.

[15] P. Sonneveld. CGS, a fast Lanczos-type solver for nonsymmetric linear systems. *SIAM J. Sci. Stat. Comput.*, 10:36–52, 1989.

[16] O. Schenk and K. Gärtner. On fast factorization pivoting methods for sparse symmetric indefinite systems. *Electronic Transactions on Numerical Analysis*, 23:158–179, 2006.

[17] Y. Okuto C. R. Crowell. Energy-Conservation Considerations in the Characterization of Impact Ionization in Semiconductors. *Phys. Rev. B*, 6:3076 – 3081, 1972.